Improved Localization of Energy Deposition in Adaptive Phased-Array Hyperthermia Treatment of Cancer

Alan J. Fenn, Vythialingam Sathiaseelan, Gerald A. King, and Paul R. Stauffer

Elevated cell tissue temperature (hyperthermia) due to radio-frequency (RF) energy absorption is known to produce an improved response for malignant tumors in humans when applied in combination with other anticancer modalities. However, clinical studies in thermotherapy have shown the difficulty of localizing RF energy deposition in malignant tissue deep within the body without damaging surrounding healthy tissue. The study presented in this article involves a preclinical investigation of adaptive feedback and computer control of amplitude and phase from coherent RF antenna arrays to provide improved distribution of electromagnetic energy deposition in the body. Measurements in a treatment-planning phantom irradiated with an adaptive antenna-array applicator show that noninvasive adaptive nulling can reduce the RF energy absorption in nearby healthy tissue while focusing energy into a deep-seated tumor site.

Over the last twenty years, many clinical studies have established that elevated cell tissue temperature (hyperthermia), induced by electromagnetic energy absorption in the radio-frequency (RF) band, significantly enhances the effect of chemotherapy and radiation therapy in the treatment of malignant tumors in the human body [1–8]. Ideally, hyperthermia treatments with RF radiating devices are administered in several treatment sessions, in which the malignant tumor is heated to a temperature above approximately 42°C for thirty to sixty minutes. Figure 1 illustrates how this hyperthermia treatment (or thermotherapy, as it is also called) is performed. During treatments with noninvasive RF applicators, clinicians have had difficulty adequately heating deep tumors while preventing surrounding healthy tissue from incurring pain and damage due to undesired hot spots greater than 44 to 45°C [9]. Two previous articles in this journal have discussed the topics of adaptive nulling and adaptive focusing [10, 11]. Since then we have significantly improved the speed of the adaptive-nulling process and expanded the scale of our experiments. This article describes a preclinical investigation of adaptively controlled phased-array transmitting antennas with multiple RF feedback sensors to provide improved distribution of electromagnetic energy deposition in malignant and healthy tissues within the body.

The electromagnetic-energy absorption rate in tissue, sometimes referred to in the literature as the SAR (specific absorption rate, or absorbed power per unit mass), has units of Joules/kg-sec (or W/kg) and may be expressed as

$$\mathrm{SAR} = \frac{1}{2}\frac{\sigma}{\rho}\left|E\right|^2, \qquad (1)$$

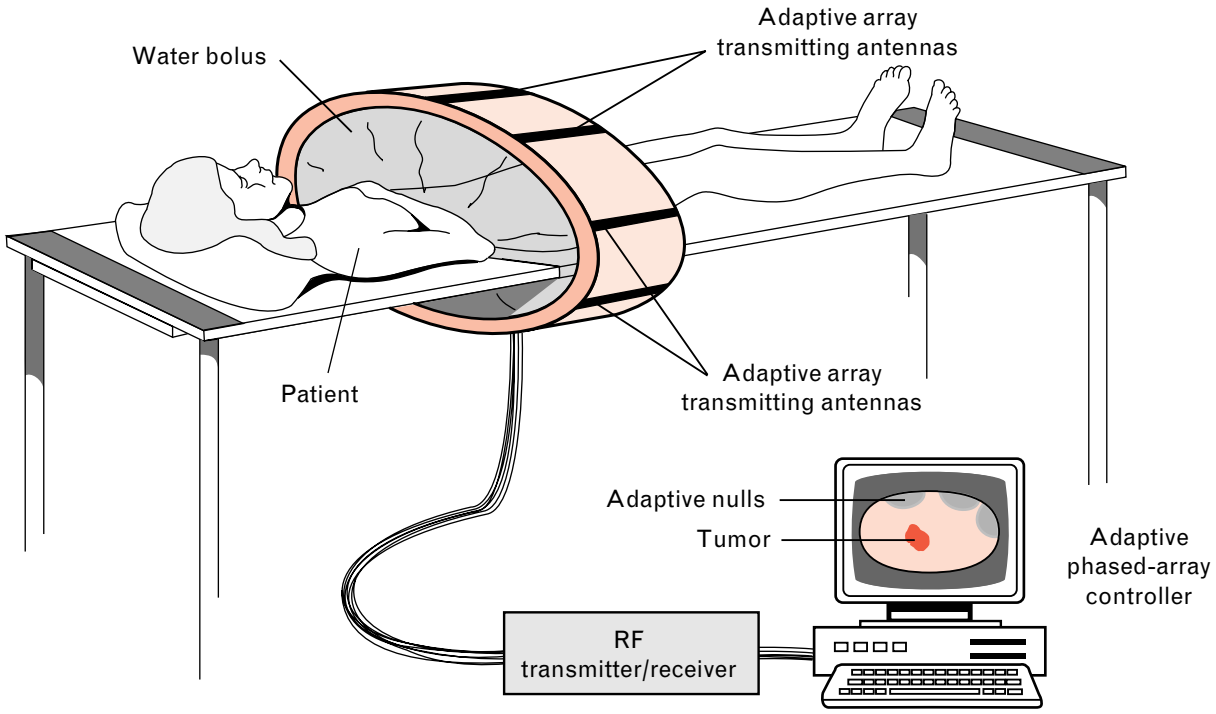

FIGURE 1. Hyperthermia treatment with radio-frequency (RF) radiating devices. A noninvasive adaptive phased-array applicator produces RF electromagnetic energy to heat deep-seated tumors in the human body. The adaptively controlled phased-array transmitting antennas, along with RF receiver feedback probes located on the skin and inside the tumor, provide improved distribution of electromagnetic-energy deposition in both malignant and healthy tissues within the body. The computer screen shows a cross section of the patient's torso with the tumor in red. Current clinical hyperthermia systems, which do not utilize adaptive phased-array techniques, produce undesired RF hot spots that can result in pain and damage to healthy tissue.

where σ is the tissue electrical conductivity (S/m), ρ is the tissue density (kg/m^3), and $|E|$ is the magnitude of the local electric field (V/m) [4]. In Equation 1, the quantity

$$\frac{1}{2}\sigma|E|^2$$

is the time-average RF power density converted to heat energy, and is called the *dissipated power*. If we ignore thermal-conduction and thermal-convection effects, which are not important until after a significant temperature rise occurs, the initial temperature rise ΔT (°C) in tissue is related to the specific absorption rate by

$$\Delta T = \frac{1}{c}\,\mathrm{SAR}\,\Delta t\,, \qquad (2)$$

where c is the specific heat of the tissue (in units of Joules/kg-°C), and Δt is the time period of exposure (sec) [4]. Substituting Equation 1 in Equation 2 yields a relation between the induced temperature rise in tissue and the applied electric field as

$$\Delta T = \frac{1}{2}\frac{\sigma}{\rho c}|E|^2\Delta t\,. \qquad (3)$$

Thus by modifying the local electric-field amplitude, we directly affect the local energy absorption and induced temperature rise in tissue. For example, in malignant tissue we would like to deposit an electric field of sufficient magnitude to heat the tumor volume to a therapeutic temperature typically in the range of 42 to 45°C. At the same time, we would like to limit the SAR magnitude in nearby healthy tissue to be less than that within the tumor in order to keep the healthy tissue temperature below approximately 44°C. Multi-element incoherent or phase-coherent

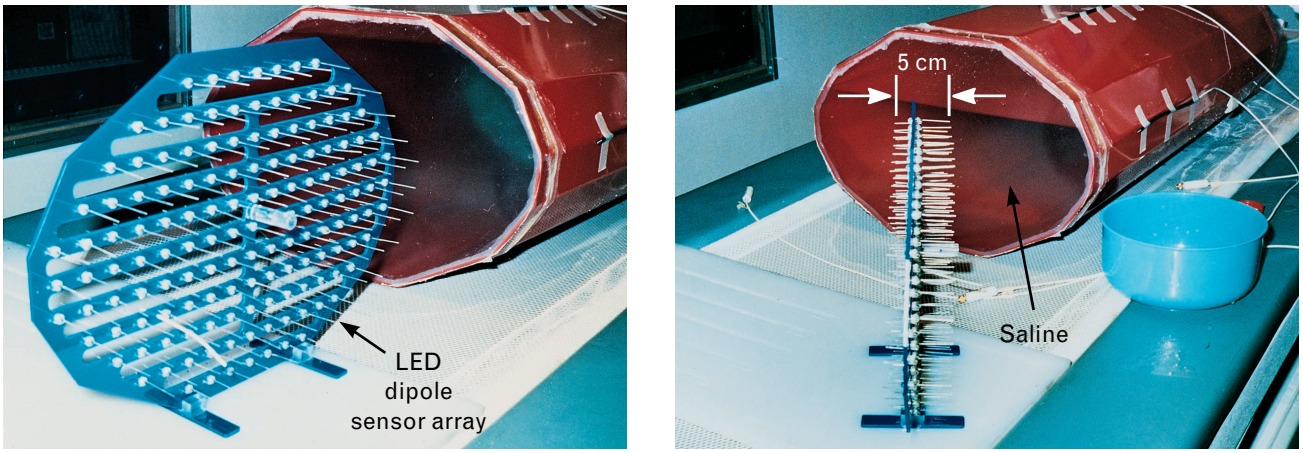

FIGURE 2. A light-emitting diode (LED) matrix phantom, which simulates a cross section of a human torso, is used in pretreatment planning for clinical hyperthermia treatments. The photographs show the LED dipole-sensor array removed from the inside of the elliptical phantom shell. The LEDs glow with an intensity proportional to the local electromagnetic field generated by a hyperthermia phased-array applicator. For treatment planning, the LED sensor array is placed inside the phantom shell and the phantom shell is filled with clear saline solution.

array antenna systems can provide significant flexibility for shaping the SAR distribution [4, 12–16].

During clinical treatments, electromagnetic radiating-array applicators have often been used in an incoherent mode, in which the power delivered to each radiating applicator is automatically adjusted on the basis of temperature-sensor feedback measurements. In many cases, incoherent 915-MHz microwave array radiation has provided effective heating of superficial tumors, but does not provide adequate heating of tumors deeper than two centimeters. In propagating through human tissue, the electric field produced by radiowave antennas attenuates rapidly, with increasing attenuation at the higher microwave frequencies. Lowering the frequency into the RF region, to below approximately 150 MHz, helps the electromagnetic wave penetrate more deeply, but still does not produce a higher value of SAR at depth compared to the value of SAR at the surface.

To increase the value of SAR at depth relative to the surface SAR, we must geometrically focus energy deposition from multiple electric fields. Because of constructive interference of electric fields at the intended focus and destructive interference of electric fields away from the focus, multichannel coherent phased-array applicators can theoretically provide deeper tissue penetration and improved localization of the absorbed energy in deep-seated tumor regions compared to incoherent array applicators [4, 14]. Unfortunately, because of complex scattering within the human body and instrumentation variations of hyperthermia phased-array system hardware [17], clinicians cannot always accurately predetermine or manually adjust the optimum settings for output power and phase of each antenna to focus heat reliably into the deep-seated tumors.

Initial investigations of nonadaptive pretreatment planning at Northwestern Memorial Hospital in Chicago used a commercial deep-heating RF phased dipole ring-array hyperthermia system [18]. The commercial ring array used for this experiment has a 60-cm diameter and normally surrounds a patient's torso. A temperature-controlled water bolus fills the region between the patient's torso and the ring array. A light-emitting diode (LED) matrix phantom, which simulates a cross section of the human torso, was constructed to display the effects of manually adjusting the amplitude and phase of the array antennas [19, 20]. Figure 2 shows the LED matrix phantom [21], which consists of 137 LED sensors positioned in an elliptically shaped Plexiglas plate with a square-grid diode spacing of 2 cm. The LED matrix is positioned within an elliptical cylinder of homogeneous saline solution contained within a 2-mm-thick hard plastic shell. The electrical conductivity of the saline is chosen to be similar to body tissues, which results

in a 100-MHz RF power-density attenuation of approximately a factor of two for each 3.0-cm distance that the RF waves propagate into the phantom. The elliptical cylinder has a cross section of 24 cm by 36 cm, similar to the cross section of a human torso, and has transparent ends for viewing the LEDs. The length of the LED metallic leads forming the dipole receive sensor is nominally 5 cm from tip to tip. The light output from the LEDs is directly proportional to the local electric-field strength generated by the RF ring array.

This LED matrix phantom has been used for pretreatment planning of nonadaptive clinical hyperthermia trials in the following manner [19]. With the matrix phantom load centered in the RF ring-array aperture, the operator begins by manually adjusting the RF power amplifiers and phase shifters until the LED phantom visually demonstrates maximum electric-field strength in the planned tumor target with as few hot spots as possible in healthy tissue, as shown in Figure 3. These manual adjustments can take over two hours to complete. Then the patient is substituted for the phantom and the clinical treatment is conducted—with the assumption that the irradiation pattern does not change substantially after the patient is substituted for the phantom. Because pretreatment planning with this manual trial-and-error adjustment procedure often produces unacceptable RF hot spots in healthy tissue for the required deep-tumor heating [19], we are now experimentally investigating pretreatment planning using much faster computer-controlled adaptive nulling [22, 23] for eliminating the unwanted hot spots in the LED phantom.

For us to localize energy deposition for an appropriate temperature rise in a deep-seated tumor, Equation 3 indicates that we must first monitor the electric-field magnitude $|E|$ received at one or more feedback probes [24] located within the tumor and adjacent healthy tissue, and then adjust the amplitude and phase of each transmitting antenna of the array for maximum RF power deposition within the tumor and minimum power deposition in nearby healthy tissue. Figure 4 illustrates the equipment setup that performs this process. A gradient-search computer algorithm that modifies antenna-array input parameters (drive signals) on the basis of the rate of change of system output parameters (power-deposition pattern) can be used to adaptively determine the individual antenna power and phase input signals to maximize (focus) or minimize (null) the electromagnetic radiation measured at one or more feedback probe positions [22, 23].

The adaptive-nulling approach used in this article is based on algorithms and testing techniques developed for adaptive phased-array radar and communications signal processing systems [25]. The resolution width of an adaptive null is approximately equal to the half-power radiation beamwidth of the adaptive-

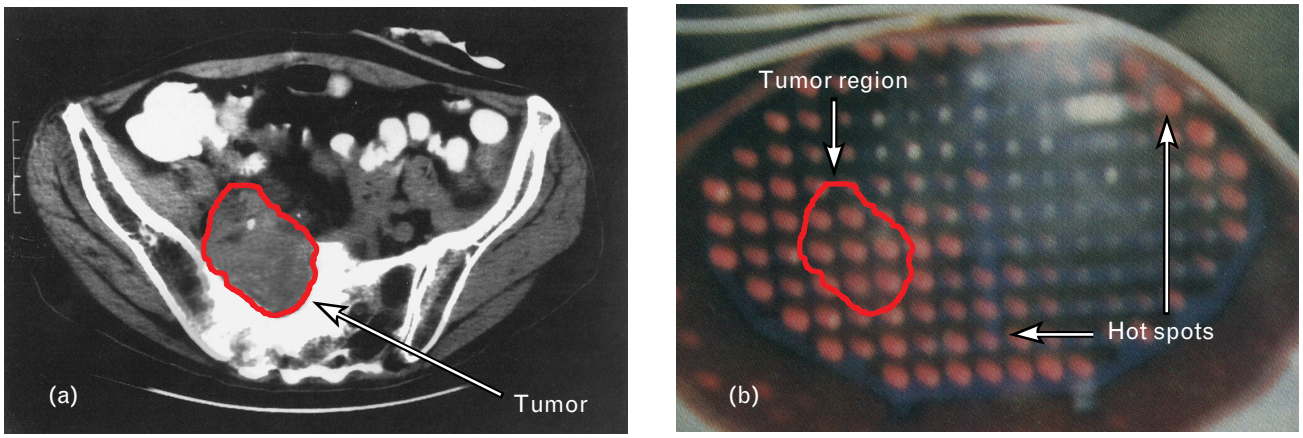

FIGURE 3. Sample nonadaptive pretreatment planning session with the LED matrix phantom. (a) The computed-tomography-scan data show the presence of a large rectal tumor. (b) After approximately two hours of manually adjusting the phase and power settings of the phased-array transmitter, the LED sensor array displays an electric-field pattern with local heating of the tumor area but with other hot spots in healthy tissue.

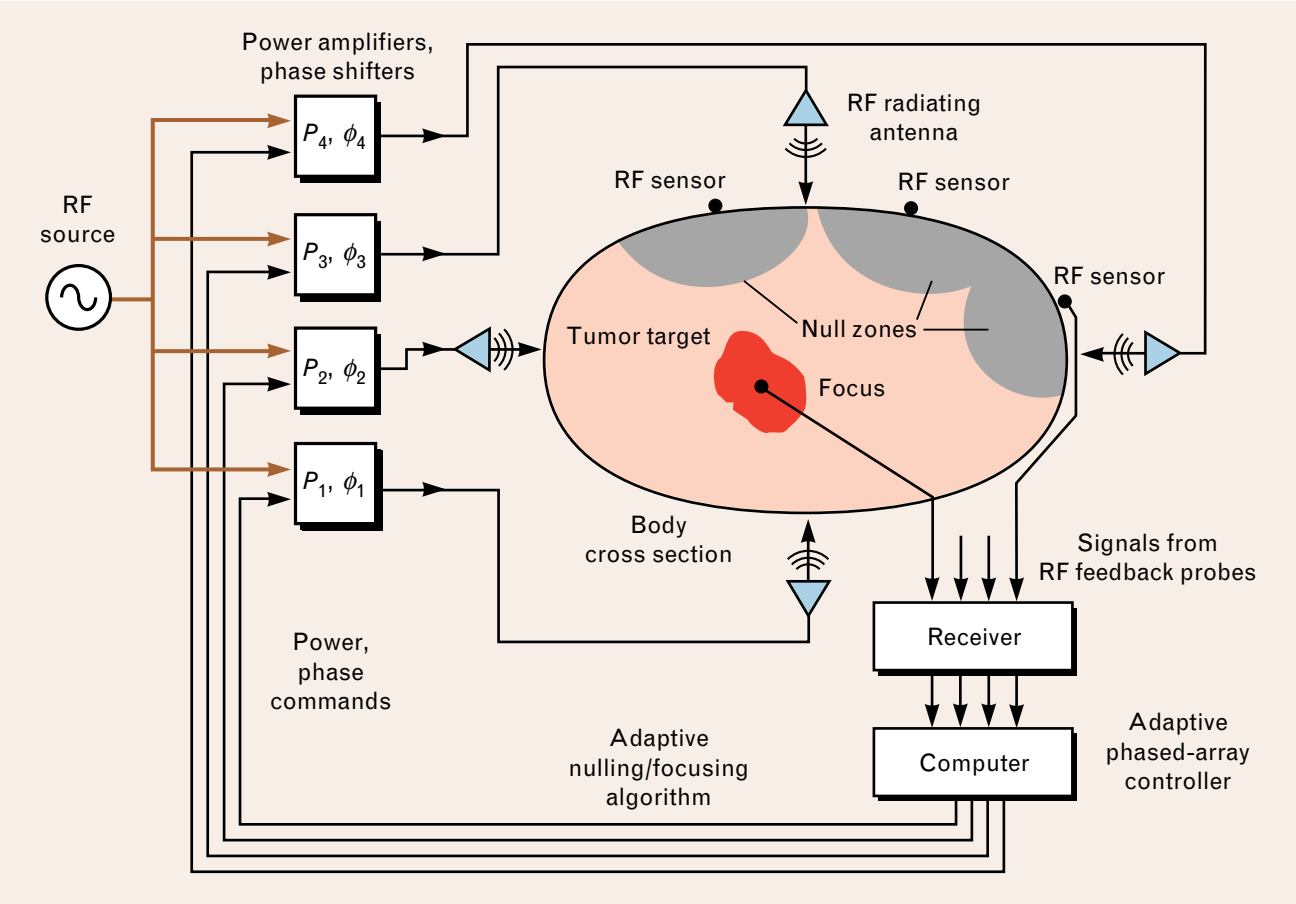

FIGURE 4. A minimally invasive system of four coherent electromagnetic radiating antennas used to heat a deep-seated malignant tumor. The RF input power and phase of each radiating antenna are computer controlled with power-deposition feedback measurements from RF feedback probes attached to the body's surface and inside the tumor. The power and phase delivered to the radiating antennas can be adjusted so that the electromagnetic radiation is simultaneously increased at the tumor and decreased at the surface sensors. At RF frequencies around 100 MHz, the nulls formed on the surface of the body are sufficiently broad (as indicated by the gray shaded regions) that nearby regions of healthy tissue within the body are protected from RF irradiation.

array antenna. This property allows an adaptive null formed on the surface of the body to reduce the electric field in regions, such as healthy tissue, that extend to some depth below the null. For hyperthermia applications, adaptive-array nulls that reduce the RF power deposition by approximately 50% or more are usually sufficient to eliminate undesired hot spots in healthy tissue.

Experimental Setup

For the current experiments, a frequency of 100 MHz was used for the ring-array system, and the sum of the input power to all four channels was held constant at 860 W. An invasive catheter with a dipole electric-field sensor one millimeter in diameter was positioned at a depth of approximately eight centimeters in the lower half of the phantom and used to measure the local electric field at the simulated deep-seated tumor site. Three independent noninvasive RF feedback probes, spaced circumferentially at ten-centimeter intervals, were attached to the surface of the phantom, as shown in Figure 5. These probes were used to measure feedback signals for reducing local power deposition on the upper surface [26].

The goal of the experiment was to irradiate only the lower portion of the phantom, which contained the simulated tumor, while minimizing irradiation of the upper portion, which contained simulated

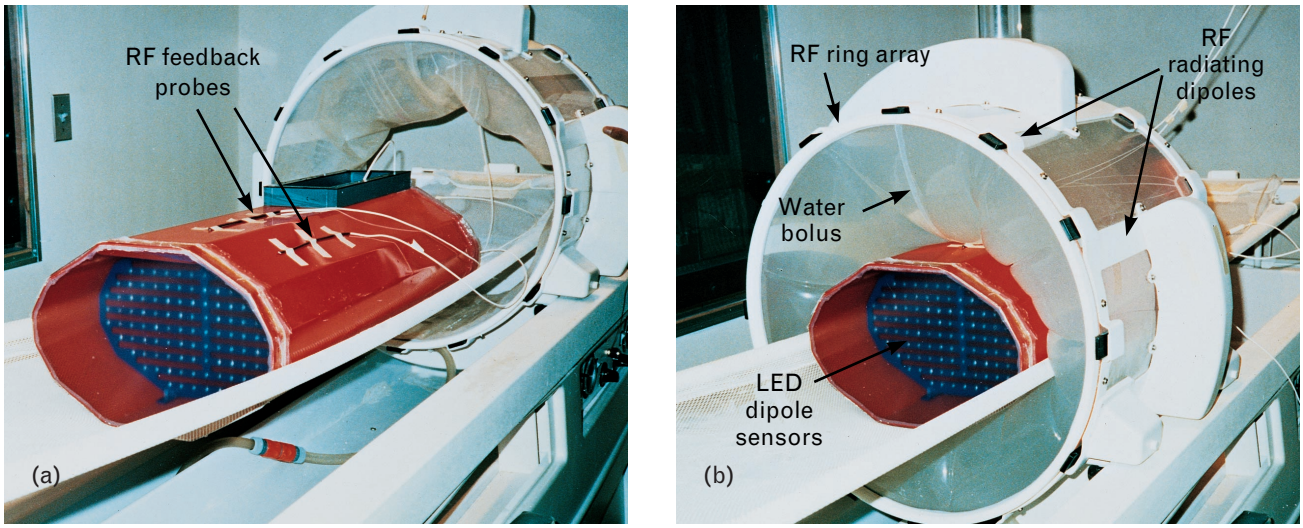

FIGURE 5. Test configuration for adaptive-nulling hyperthermia phased-array experiments. (a) LED matrix phantom with RF feedback probes mounted on the surface of the phantom. (b) The LED phantom is placed within the RF ring array and the water bolus is filled. The adaptive-nulling phased array consists of four active transmit channels, each connected to a pair of RF radiating dipoles.

healthy tissue. At 100 MHz, the RF wavelength in the saline phantom is approximately thirty centimeters. The half-power beamwidth (or null width) of an adaptive ring array is approximately equal to one-half the wavelength, or fifteen centimeters. Thus an intense null formed on the surface of the phantom should reduce the electric field by about 50% at a depth of fifteen centimeters. Less intense surface nulls would have less effect on reducing the electric-field intensity at depth.

The input power and phase delivered to each of the four RF radiating dipole pairs of the ring array were manually set to equal initial values of 215 W and 90°, respectively. The computer, as illustrated in Figure 4, started the adaptive-array algorithm by automatically adjusting, via digital-to-analog converters, the power amplifiers and phase shifters in each of the four channels of the phased array. The computer software performed calculations of the rate of change of the measured RF power at the surface sensors (simulated healthy tissue regions) after each adjustment of RF power and phase to the array transmit channels. For this experiment we used a modified method-of-steepest-descent algorithm to determine the input power and phase commands that minimize the summation of the local power deposition measured by each surface RF feedback sensor. All adjustments were completed and the adaptive nulls were formed in approximately two minutes, which is an appropriate speed for real-time use in optimizing clinical treatments.

Before adaptive nulling, both the RF feedback sensors and the LED phantom indicated multiple hot spots. The light-toned bars in Figure 6 indicate the measured RF feedback data before adaptive nulling, and the light-intensity pattern in the photograph in Figure 7(a) indicates the associated deposition of RF energy, including hot spots. Then the adaptive-nulling algorithm was executed for three iterations to reduce the RF feedback signal at each surface-nulling sensor by at least a factor of two. The RF feedback sensors and the LED phantom then displayed the electric-field distributions after adaptive nulling, as shown by the dark-toned bars in Figure 6 and the light-intensity pattern in Figure 7(b). The simulated tumor position in the lower half of the phantom is fully irradiated while the upper half of the phantom, containing the region of simulated healthy tissue, has a substantially reduced electric-field intensity.

We then ran a second experiment to attempt to null the electric field noninvasively over the right half of the phantom, rather than the upper half. Figure 8 shows the measured RF feedback data before and after nulling. As in the first experiment, adaptive nulling significantly increases the RF power deposited in

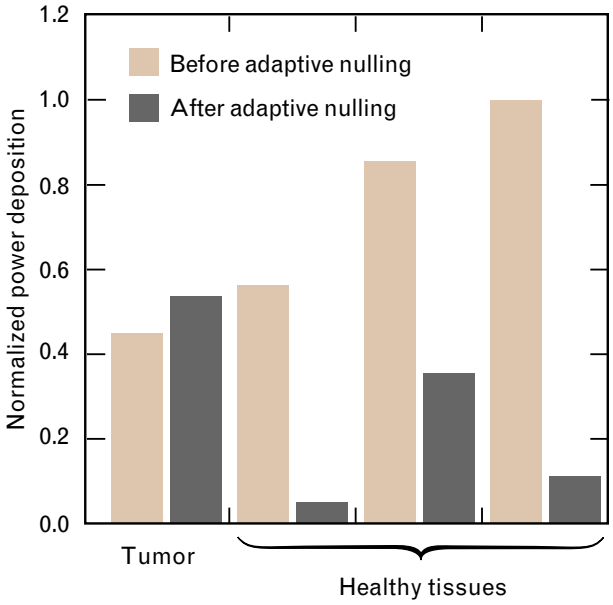

FIGURE 6. Measured electric-field probe data in a pretreatment-planning phantom. These data demonstrate the effect of adaptive nulling at three independent surface sites. The adaptive nulling protects regions of healthy tissue while an 8-cm-deep tumor site is irradiated with a coherent four-channel ring phased-array system operating at a radio frequency of 100 MHz. The light-toned bars indicate the normalized RF power deposition at each electric-field sensor before adaptive nulling. The RF power deposition in healthy tissue, prior to adaptive nulling, is greater than the RF power deposition in the tumor. The RF power deposition after adaptive nulling, indicated by the dark-toned bars, measured at the simulated deep-seated tumor site increases by 19%, while the RF power deposition measured by the three electric-field feedback probes on the surface of the phantom is reduced by 91%, 57%, and 87%, respectively. The measurements demonstrate that the adaptive-nulling process results in a stronger irradiation of the tumor compared to the irradiation of the superficial healthy tissue.

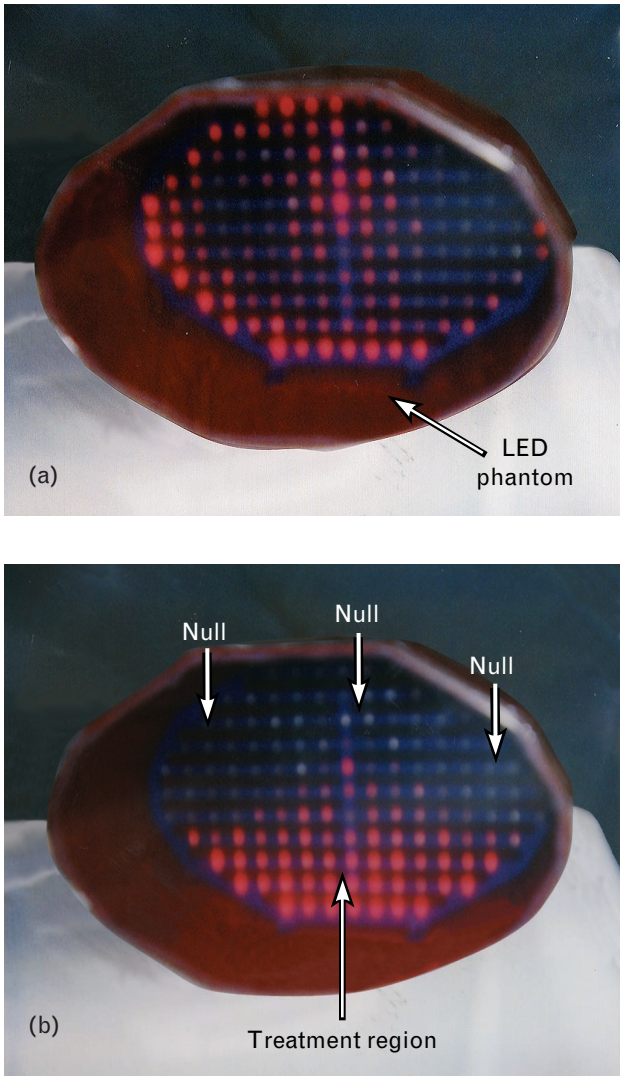

FIGURE 7. Pretreatment-planning LED matrix phantom irradiated by an adaptively controlled coherent RF ring array operating at 100 MHz. (a) Before adaptive nulling the light-intensity pattern of the two-dimensional LED display reveals hot spots along the top, bottom, and left and right surfaces of the phantom as well as in the central region. (b) After adaptive nulling at three positions on the upper-half surface of the phantom, the RF irradiation is concentrated over the lower portion of the phantom (the position of the simulated tumor), while irradiation of the upper portion of the phantom (the position of healthy tissue) is significantly reduced. The experiment shows that the effect of the noninvasive adaptive-nulling process is to shift the RF irradiation away from the healthy tissue areas and toward the tumor.

the tumor site while significantly decreasing the power delivered to the healthy tissue sites. Figure 9 shows photographs of the phantom before nulling and after the nulling algorithm has converged. These data clearly show that it is possible to restrict the heating to the left side of the target body.

In order to protect large volumes of healthy tissue while focusing RF energy deep within the body, we must have the essential ability to produce multiple electric-field minima. Fortunately, these minima can be easily generated by using noninvasive RF feedback probes located on the tissue surface near each desired electric-field minimum. Our measurements in a simple homogeneous LED phantom indicate that we

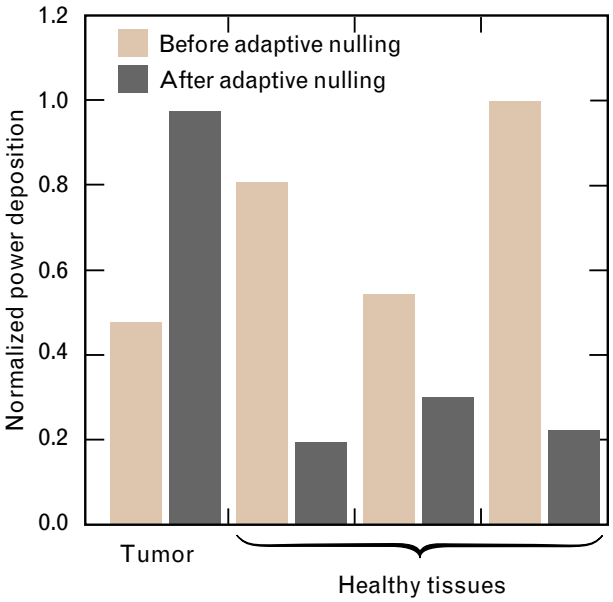

FIGURE 8. Measured RF feedback data before and after nulling (second experiment). The normalized RF power deposition after adaptive nulling, indicated by the dark bars, measured at the simulated deep-seated tumor site increases by 106%, while the RF power deposition measured by the three feedback probes on the surface of the phantom is reduced by 77%, 45%, and 78%, respectively.

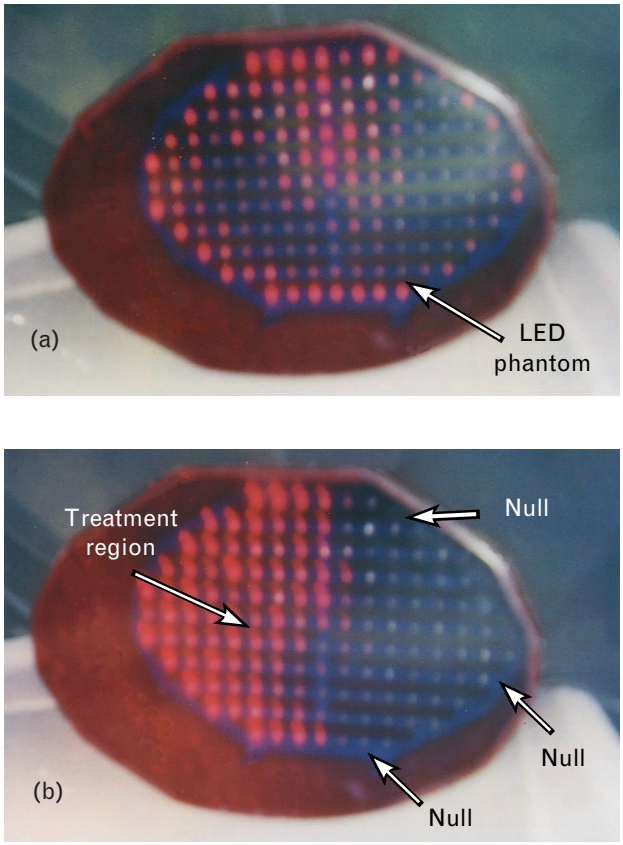

FIGURE 9. Pretreatment-planning LED matrix phantom irradiated by an adaptively controlled coherent RF ring array operating at 100 MHz. (a) Before adaptive nulling, the light-intensity pattern of the two-dimensional diode display reveals hot spots along the top, bottom, and left and right surfaces of the phantom as well as in the central region. (b) After adaptive nulling at three positions on the right-half surface of the phantom, the RF irradiation is concentrated over the left portion of the phantom (site of the simulated tumor position), while irradiation of the right portion (simulating healthy tissue) is significantly reduced. As in Figure 7, the experiment shows that the effect of the noninvasive adaptive-nulling process is to shift the RF irradiation away from the areas of healthy tissue and toward the tumor.

can adaptively control the transmit power and phase distributions in an electromagnetic hyperthermia phased-array system, and thus optimize the RF power-deposition distribution prior to treatment by using a treatment-planning phantom. In addition to the control of power-deposition distributions by adaptive-array phase and power adjustments with RF feedback as reported here, subsequent minor adjustments of temperature in a perfused tumor can be made during the clinical treatments by using local temperature feedback measurements to adaptively control the total power delivered to the hyperthermia applicator as a function of time [27, 28].

Conclusion

An adaptive power-deposition feedback and control technique has been investigated experimentally in two dimensions with an LED matrix phantom and an electromagnetic four-channel dipole-array hyperthermia system with adjustable amplitude and phase. The measured data demonstrate that the distribution of electromagnetic-energy absorption generated by a hyperthermia phased-array applicator can be improved by an adaptive-nulling feedback and control algorithm with multiple independent RF feedback probes. Further investigation of this adaptive phased-array control procedure should be initiated for improving the localization of heating in deep-seated tumors by providing real-time compensation for variable blood flow.

Acknowledgments

We would like to thank Alden Hayashi for a critical review of the manuscript. The support of the Lincoln Laboratory Advanced Concepts Committee is sincerely appreciated. The authors are grateful to D.H. Temme of Lincoln Laboratory for technical discussions. This work was sponsored by the Department of the Air Force.

REFERENCES

1. P.K. Sneed and T.L. Phillips, "Combining Hyperthermia and Radiation: How Beneficial?" *Oncology* **5,** Mar. 1991, pp. 99–108.
2. E.J. Hall, *Radiobiology for the Radiologist* (Lippincott, Philadelphia, 1994), chap. 16.
3. J. Overgaard, D. Gonzales Gonzalez, M.C.C.H. Hulshof, G. Arcangeli, O. Dahl, O. Mella, and S.M. Bentzen, "Hyperthermia as an Adjuvant to Radiation Therapy of Recurrent or Metastatic Malignant Melanoma. A Multicentre Randomized Trial by the European Society for Hyperthermic Oncology," *Int. J. Hyperthermia* **12** (1), 1996, pp. 3–20.
4. S.B. Field and J.W. Hand, eds., *An Introduction to the Practical Aspects of Clinical Hyperthermia* (Taylor & Francis, London, 1990).
5. P. Fessenden and J.W. Hand, in *Medical Radiology: Radiation Therapy Physics*, A.R. Smith, ed. (Springer-Verlag, Berlin, 1995), pp. 315–363.
6. M.H. Seegenschmiedt, P. Fessenden, and C.C. Vernon, eds., *Thermoradiotherapy and Thermochemotherapy* **1**: *Biology, Physiology, Physics* (Springer-Verlag, Berlin, 1995).
7. C.A. Perez, B. Emami, R.J. Myerson, and J.L. Roti Roti, in *Principles and Practice of Radiation Oncology*, C.A. Perez and L.W. Brady, eds. (Lippincott, Philadelphia, 1992), chap. 16.
8. K. Sugimachi, H. Kuwano, H. Ide, T. Toge, M. Saku, and Y. Oshiumi, "Chemotherapy Combined with or without Hyperthermia for Patients with Oesophageal Carcinoma: A Prospective Randomized Trial,'' *Int. J. Hyperthermia* **10** (4), 1994, pp. 485–493.
9. J.W. Strohbehn, "Hyperthermia Equipment Evaluation," *Int. J. Hyperthermia* **10** (3), 1994, pp. 429–432.
10. A.J. Fenn and G.A. King, "Adaptive Nulling in the Hyperthermia Treatment of Cancer," *Linc. Lab. J.* **5** (2), 1992, pp. 223–240.
11. A.J. Fenn, C.J. Diederich, and P.R. Stauffer, "An Adaptive Focusing Algorithm for a Microwave Planar Phased-Array Hyperthermia System," *Linc. Lab. J.* **6** (2), 1993, pp. 269–288.
12. W. Gee, S.-W. Lee, N.K. Bong, C.A. Cain, R. Mittra, and R.L. Magin, "Focused Array Hyperthermia Applicator: Theory and Experiment," *IEEE Trans. Biomed. Eng.* **31** (1), 1984, pp. 38–46.
13. C.J. Diederich and P.R. Stauffer, "Pre-Clinical Evaluation of a Microwave Planar Array Applicator for Superficial Hyperthermia," *Int. J. Hyperthermia* **9** (2), 1993, pp. 227–246.
14. P.F. Turner, "Mini-Annular Phased Array for Limb Hyperthermia," *IEEE Trans. Microw. Theory Tech.* **34** (5), 1986, pp. 508–513.
15. E.R. Lee, T.R. Wilsey, P. Tarczy-Hornoch, D.S. Kapp, P. Fessenden, A. Lohrbach, and S.D. Prionas, "Body Conformable 915 MHz Microstrip Array Applicators for Large Surface Area Hyperthermia," *IEEE Trans. Biomed. Eng.* **39** (5), 1992, pp. 470–483.
16. M.K. Gopal, J.W. Hand, M.L.D. Lumori, S. Alkhairi, K.D. Paulsen, and T.C. Cetas, "Current Sheet Applicator Arrays for Superficial Hyperthermia of Chestwall Lesions," *Int. J. Hyperthermia* **8** (2), 1992, pp. 227–240.
17. P. Wust, H. Fähling, R. Felix, S. Rahman, R.D. Issels, H. Feldmann, G. van Rhoon, and J. van der Zee, "Quality Control of the SIGMA Applicator Using a Lamp Phantom: A Four-Centre Comparison," *Int. J. Hyperthermia* **11** (6), 1995, pp. 755–768.
18. P.F. Turner, T. Schaefermeyer, and T. Saxton, "Future Trends in Heating Technology of Deep-Seated Tumors," *Recent Results in Cancer Research* **107,** 1988, pp. 249–262. Our group modified the software that controls the transmitter RF power and phase in each channel of the array, allowing the adaptive nulling experiments to be conducted.
19. B.B. Mittal, V. Sathiaseelan, R.M. Shetty, K.D. Kiel, M.C. Pierce, W. Adelman, and M.H. Marymont, "Regional Hyperthermia in Patients with Advanced Malignant Tumors: Experience with the BSD 2000 Annular Phased-Array System and Sigma 60 Applicator," *Endocurietherapy/Hyperthermia Oncology* **10,** 1994, pp. 223–236.
20. C. Schneider and J.D.P. van Dijk, "Visualization by a Matrix of Light-Emitting Diodes of Interference Effects from a Radiative Four-Applicator Hyperthermia System," *Int. J. Hyperthermia* 7 (2), 1991, pp. 355–366.
21. C.J. Schneider, J.D.P. van Dijk, A.A.C. De Leeuw, P. Wust, and W. Baumhoer, "Quality Assurance in Various Radiative Hyperthermia Systems Applying a Phantom with LED Matrix," *Int. J. Hyperthermia* **10** (5), 1994, pp. 733–747.
22. A.J. Fenn and G.A. King, "Experimental Investigation of an Adaptive Feedback Algorithm for Hot Spot Reduction in Radio-Frequency Phased-Array Hyperthermia," *IEEE Trans. Biomed. Eng.* **43** (3), 1996, pp. 273–280.
23. A.J. Fenn and G.A. King, "Adaptive Radio-Frequency Hyperthermia Phased-Array System for Improved Cancer Therapy: Phantom Target Measurements," *Int. J. Hyperthermia* **10** (2), 1994, pp. 189–208.
24. Miniature electric-field measurement probes with a diameter equal to 1 mm are commercially available for clinical use. These probes can fit inside standard implantable catheters. See M. Astrahan et al., "Heating Characteristics of a Helical Microwave Applicator for Transurethral Hyperthermia of Benign Prostatic Hyperplasia," *Int. J. Hyperthermia*, 7 (1), 1991, pp. 141–155.
25. R.A. Monzingo and T.W. Miller, *Introduction to Adaptive Arrays* (Wiley, New York, 1980), chap. 4.
26. With a four-channel phased array system, it is possible to form as many as three independent nulls. To form more than three independent nulls it is necessary to utilize an increased number of transmitter channels.
27. A. Hartov, T.A. Colacchio, J.W. Strohbehn, T.P. Ryan, and P.J. Hoopes, "Performance of an Adaptive MIMO Controller for a Multiple-Element Ultrasound Hyperthermia System," *Int. J. Hyperthermia* **9** (4), 1993, pp. 563–579.
28. W.-L. Lin, R.B. Roemer, and K. Hynynen, "Theoretical and Experimental Evaluation of a Temperature Controller for Scanned Focused Ultrasound Hyperthermia," *Med. Phys.* **17** (4), 1990, pp. 615–625.

ALAN J. FENN
is an assistant leader in the RF Technology group. He received a B.S. degree from the University of Illinois in Chicago, and M.S. and Ph.D. degrees from The Ohio State University, all in electrical engineering. He joined the staff of Lincoln Laboratory in 1981 and was a member of the Space Radar Technology group from 1982 to 1991, where his research was in phased-array antenna design, adaptive-array near-field testing, and antenna and radar cross-section measurements. Since 1990 he has conducted research in the application of adaptive-nulling techniques to radio-frequency hyperthermia treatment. He is currently investigating optically controlled phased-array antennas for mobile satellite communications applications.

In 1990 Alan was a corecipient of the IEEE Antennas & Propagation Society's H.A. Wheeler Applications Prize Paper Award for "Phased Array Antenna Calibration and Pattern Prediction Using Mutual Coupling Measurements," a paper that he coauthored for the *IEEE Transactions on Antennas and Propagation.* He is a senior member of the IEEE, a member of the North American Hyperthermia Society, and an associate member of the American Society for Therapeutic Radiology and Oncology. He has also been appointed to a five-year term of membership in the Institute for Systems and Components of the Electromagnetics Academy.

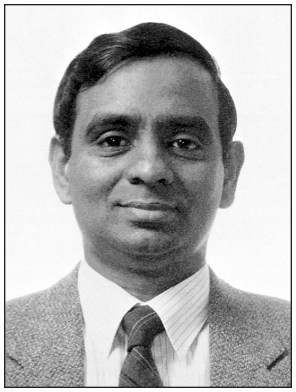

VYTHIALINGAM SATHIASEELAN
received a B.Sc. degree in electronics engineering from the University of Sri Lanka in 1976 with First Class honors, and the Ph.D. degree in microwave engineering from the University of Bradford in 1982. In 1975 he received the UNESCO Team Gold Medal as the best engineering student, and the Dr. O.P. Kulshresha Silver Medal as the best engineering student among the electrical power and electronics groups. From 1982 to 1986 he was a research scientist with the Medical Research Council's Clinical Oncology and Radiotherapeutics Unit in Cambridge, England. He was an assistant professor in the Washington University School of Medicine from 1986 to 1988. He is currently employed by Northwestern Memorial Hospital as a hyperthermia engineer in the Radiation Oncology Center. He also holds an appointment as assistant professor in clinical radiology at Northwestern University Medical School. He is a member of several professional societies, including the Institution of Electrical and Electronics Engineers, the American Association of Physicists in Medicine, the North American Hyperthermia Society, and the American Society for Therapeutic Radiology and Oncology. He is the author or coauthor of thirty-five articles in his field, and he has presented twenty-five papers at national and international society meetings.

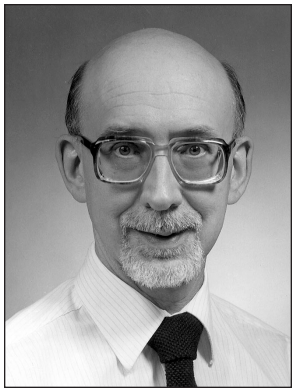

GERALD A. KING
studied electrical engineering and biology at the Rensselaer Polytechnic Institute, and was a research fellow at the State University of New York (SUNY) Upstate Medical Center in Syracuse, New York, where he received an M.D. degree in 1965. He completed his internship at St. Joseph's Hospital in Syracuse and his residency at the Stanford University Medical Center in Palo Alto, California. From 1969 to 1971, he was the chief of radiation therapy service and director of residency training for radiation therapy at the Fitzsimmons General Hospital in Denver. In 1971, he returned to Syracuse, where he has been an attending radiation oncologist at the University Hospital, SUNY Health Science Center; the Veterans Administration Hospital; and the Crouse Irving Memorial Hospital. He is now the Associate Director of the Division of Radiation Oncology, University Hospital, SUNY Health Science Center in Syracuse, and the Director of the hospital's Hyperthermia Cancer Treatment and Research Center. He is also a professor in the SUNY Health Science Center's Department of Radiology in the College of Medicine. An associate editor of *Medical Physics,* he is the author or coauthor of more than thirty articles in his field and has presented nearly fifty papers at national and international society meetings.

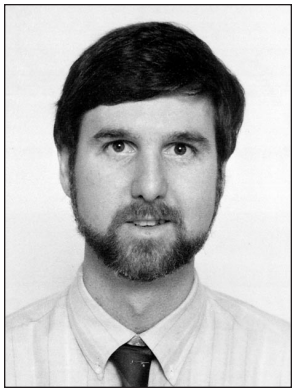

PAUL R. STAUFFER
received a B.A. degree in physics from the College of Wooster in 1975 and an M.S. degree in electrical engineering from the University of Arizona in 1979. Additional specialization in clinical engineering led to a position as research associate in the Division of Radiation Oncology at the University of Arizona from 1979 to 1983. He received board certification in Clinical Engineering in 1983, and board cerftification in Medical Physics in 1991. He is currently an associate professor in the Department of Radiation Oncology at the University of California, San Francisco, where his focus of research continues to be the engineering development and testing of improved RF, microwave, and ultrasound technologies for hyperthermia and thermal therapy applications. He is a member of the North American Hyperthermia Society, IEEE, Association of the Advancement of Medical Instrumentation, and the American Association of Physicists in Medicine. He has published over seventy papers, reports, and book chapters in the field of hyperthermia, and is associate editor for the *International Journal of Hyperthermia* and the *International Journal of Radiation Oncology, Biology, and Physics*.